Experimental-numerical determination of the Taylor-Quinney coefficient

J. Johnsen[1], L.E.B. Dæhli[2], T. Børvik[2,3], O.S. Hopperstad[2,3]

[1]Enodo AS, Trondheim, Norway
[2]Structural Impact Laboratory (SIMLab), Department of Structural Engineering, Norwegian University of Science and Technology (NTNU), Trondheim, Norway
[3]Centre for Advanced Structural Analysis (SFI CASA), Department of Structural Engineering, NTNU, Trondheim, Norway

Abstract

During plastic deformation of a metal, a part of the plastic work is stored in the material due to local distortion of the crystal lattice, while the remainder is dissipated as heat. The part of the plastic work dissipated as heat can be observed on a macroscopic scale through thermal measurements in high strain rate experiments. Typically, this fraction of plastic work converted into heat is assumed to be constant and around 90%. In this study, we have performed tension tests at a constant crosshead velocity of 0.6 mm/s on flat notched specimens from a DP600 steel material. Digital image correlation (DIC) was used to apply virtual extensometers spanning the length of the notched area. Furthermore, an infrared camera was used to measure the temperature increase over the same area as monitored by DIC, enabling correlation between temperature and displacement. These temperature-displacement curves were used as the target curves in thermomechanical simulations to obtain the Taylor-Quinney coefficient as a function of the equivalent plastic strain. It was found that the Taylor-Quinney coefficient exhibits quite large variations during the experiment, ranging from a minimum of about 0.5 in the beginning of the test, to about 0.95 at the end of test.

1 Introduction

During high-rate loading, the material undergoes extensive heating due to the plastic work dissipated under nearly adiabatic conditions. The plastic work consists of two parts – the amount dissipated as heat, and an amount stored as elastic energy due to the generation of dislocations. The fraction of plastic work dissipated as heat is frequently referred to as the Taylor-Quinney coefficient (β). In the literature, the Taylor-Quinney coefficient is typically assumed to be constant and equal to $\beta = 0.9$. In reality, β is not a constant but varies with work hardening, strain rate, and temperature, because these parameters affect the rate at which dislocations are stored and annihilated. This was shown in the seminal paper by Taylor and Quinney [1], where they observed that the amount of latent heat decreased as a function of deformation for both annealed mild steel and decarburized mild steel. The variation of the Taylor-Quinney coefficient under different loading conditions has been studied by several authors, see e.g. [2-6].

In this study, we have performed experiments on notched tension specimens of a 1.0 mm thick DP600 steel sheet material. The notched tension test was instrumented with a digital camera and an infrared camera for full-field measurements of the displacement and temperature fields, respectively, at the specimen surface. This enables a correlation between the temperature increment and the local deformation within the notch region of the specimen. The temperature versus displacement curves from these tests were then used to determine the variation of the Taylor-Quinney coefficient by an inverse modelling approach using thermomechanical finite element simulations in LS-DYNA together with a user subroutine to control the Taylor-Quinney coefficient. Finally, it is shown that the proposed experimental-numerical approach to determine the evolution of the Taylor-Quinney coefficient gives an excellent agreement between the measured and the simulated temperature evolution in the notched specimen.

2 Experiments

The experiments were conducted in an Instron 5982 (100 kN) universal testing machine. The notched tension (NT3) specimens (Figure 1) were loaded using a constant crosshead velocity of 0.6 mm/s.

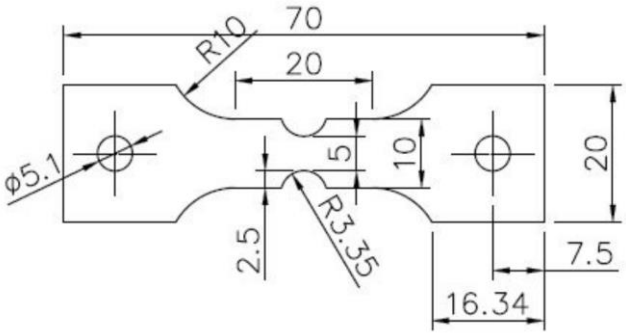

Fig.1: Dimensions of the notched tension (NT3) specimens with a thickness of 1.0 mm. All measures are in mm.

A Basler ac4112-30um area scan camera with a 100 mm macro lens captured 5 frames per second (fps) of the surface of the specimen during loading, while a FLIR SC 7500 thermal camera operating at 200 fps was used to capture the temperature increase on the opposite surface of the specimen, see Figure 2.

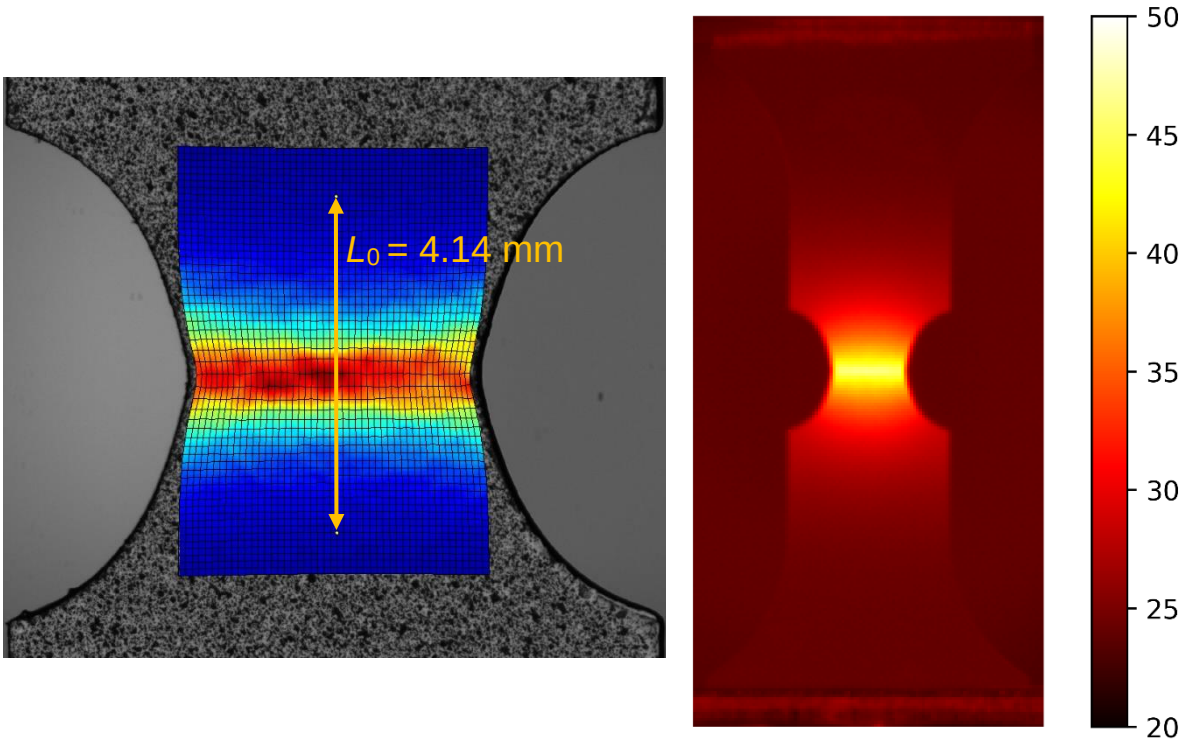

(a) (b)

Fig.2: (a) The maximum principal strain just before fracture together with the virtual extensometer, and (b) the temperature in degree Celsius on the opposite surface of the specimen just before failure.

The time series from the two cameras were correlated after the tests, which enabled us to express the maximum temperature increase on the surface of the specimen as a function of the engineering strain, see Figure 3.

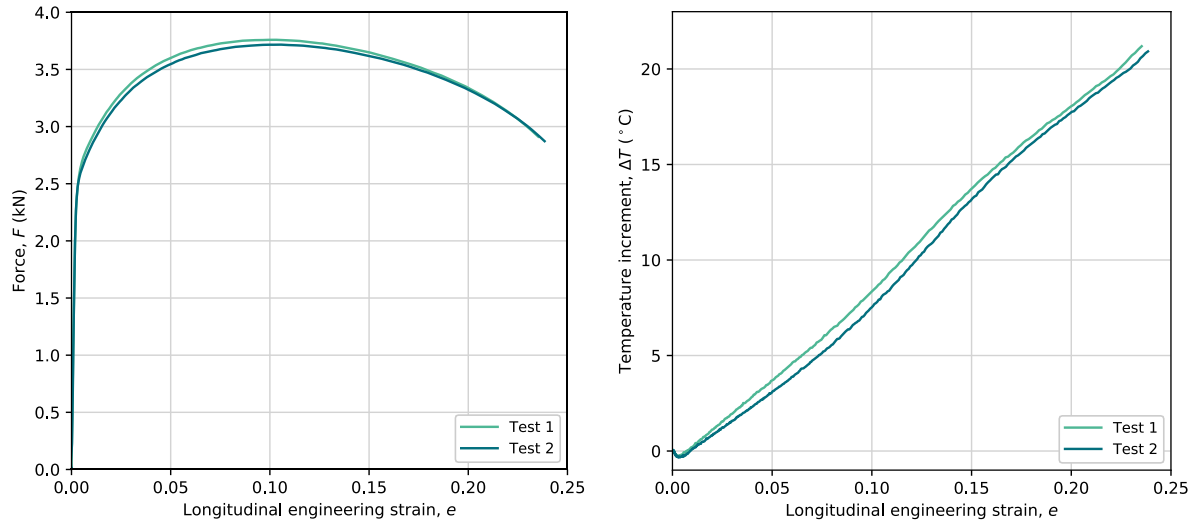

(a) (b)

Fig.3: (a) Force and (b) temperature increment versus engineering strain from the two test repetitions.

The laser flash method [7] was used to establish the specific heat capacity (c_v) and thermal conductivity (k) given in Table 1, while the remaining material parameters were taken from literature.

Table 1: Material parameters for the DP600 sheet material.

Density, ρ (kg/m^3)	Young's modulus E (MPa)	Poisson's ratio, ν	Specific heat capacity, c_v (J/(kg·K))	Thermal conductivity, k (W/(m^2·K))	Thermal expansion coefficient, α_T (K^{-1})
7850.0	210,000	0.3	420	44.6	$1.0 \cdot 10^{-5}$

3 Constitutive model

We use a hypoelastic formulation of the constitutive model and an additive decomposition of the corotational rate-of-deformation tensor $\widehat{\mathbf{D}}$ into elastic and plastic parts is thus assumed

$$\widehat{\mathbf{D}} = \widehat{\mathbf{D}}^{\mathrm{e}} + \widehat{\mathbf{D}}^{\mathrm{p}} \tag{1}$$

The material is modelled as isotropic and linearly thermo-elastic according to Hooke's law on rate form, viz.

$$\hat{\boldsymbol{\sigma}} = 2\mu \mathrm{dev}\left(\widehat{\mathbf{D}}^{\mathrm{e}}\right) + \kappa\left(\mathrm{tr}\left(\widehat{\mathbf{D}}^{\mathrm{e}}\right) - 3\alpha_{\mathrm{T}}\dot{T}\right)\mathbf{1} \tag{2}$$

where $\hat{\boldsymbol{\sigma}}$ is the corotated Cauchy stress tensor, μ and κ are the shear and bulk moduli, α_{T} and $\dot{T}$ are the thermal expansion coefficient and the temperature rate, $\mathbf{1}$ is the second order identity tensor, and $\mathrm{dev}(\mathbf{X})$ and $\mathrm{tr}(\mathbf{X})$ denote the deviatoric and spherical part of the tensor $\mathbf{X}$, respectively. The yield function is given by

$$f = \sigma_{\mathrm{eq}}(\hat{\boldsymbol{\sigma}}) - \left(\sigma_0 + R(p)\right)\left(1 - (T^*)^m\right) \leq 0 \tag{3}$$

where σ_{eq} is the Hershey-Hosford [8,9] equivalent stress, viz.

$$\sigma_{\mathrm{eq}} = \left[\frac{1}{2}\left(|\sigma_1 - \sigma_2|^a + |\sigma_2 - \sigma_3|^a + |\sigma_3 - \sigma_1|^a\right)\right]^{\frac{1}{a}} \tag{4}$$

where σ_i are the principal stresses and a is a positive integer, which we set to a value of $a = 6$ in the numerical simulations. The homologous temperature T^* is defined as

$$T^* = \frac{T - T_0}{T_{\mathrm{m}} - T_0} \tag{5}$$

where T is the temperature and T_0 and T_m are the initial and melting temperature, respectively. The initial yield stress at $T = T_0$ is defined by σ_0, whereas the parameter m governs the temperature sensitivity of the material. The work hardening is defined by

$$R(p) = \sum_{i=1}^{3} Q_i(1 - \exp(-C_i p)) \tag{6}$$

where p is the equivalent plastic strain, and Q_i and C_i are hardening parameters.

The corotated plastic rate-of-deformation tensor $\widehat{\mathbf{D}}^{\mathrm{p}}$ is obtained from the associative flow rule

$$\widehat{\mathbf{D}}^{\mathrm{p}} = \dot{p}\frac{\partial f}{\partial \hat{\boldsymbol{\sigma}}} \tag{7}$$

where the equivalent plastic strain rate $\dot{p}$ is defined from the viscoplastic constitutive relation

$$\dot{p} = \begin{cases} 0 & \text{if} \quad f \le 0 \\ \dot{p}_0 \left[\left(\dfrac{\sigma_{\mathrm{eq}}}{(\sigma_0 + R(p))(1 - (T^*)^m)} \right)^{\frac{1}{C}} - 1 \right] & \text{if} \quad f > 0 \end{cases} \tag{8}$$

Here, $\dot{p}_0$ is a reference equivalent plastic strain rate and C is a rate-sensitivity parameter. In the plastic domain, the equivalent stress is then given as

$$\sigma_{\mathrm{eq}} = (\sigma_0 + R(p))\left(1 + \frac{\dot{p}}{\dot{p}_0}\right)^{C}(1 - (T^*)^m) \tag{9}$$

which is recognized as a modified Johnson-Cook equivalent stress [10]. The current temperature T is obtained from the heat equation as

$$\rho c_{\mathrm{v}}\dot{T} = \beta\sigma_{\mathrm{eq}}\dot{p} + k\Delta T - 3\kappa\alpha_{\mathrm{T}}T\mathrm{tr}\left(\widehat{\mathbf{D}}^{\mathrm{e}}\right) \tag{10}$$

where Δ is the Laplacian operator. Note that external heat sources are excluded in the local energy balance to arrive at this expression.

The parameters used in the constitutive model are given in Table 2.

Table 2: Material parameters used in the constitutive model.

Yielding and work hardening							Viscoplasticity		
σ_0 (MPa)	Q_1 (MPa)	C_1 (-)	Q_2 (MPa)	C_2 (-)	Q_3 (MPa)	C_3 (-)	C (-)	$\dot{p}_0$ (1/s)	m (-)
346.77	184.76	163.651	269.23	9.733	302.1	0.515	0.005	0.001	1

4 Numerical optimization of the Taylor-Quinney coefficient

Using a user subroutine, the Taylor-Quinney coefficient was tabulated as a piecewise linear function of the equivalent plastic strain. The initial values of the coefficients governing the piecewise linear function were estimated by running a series of thermo-coupled FE simulations (Figure 4) with a constant Taylor-Quinney coefficient.

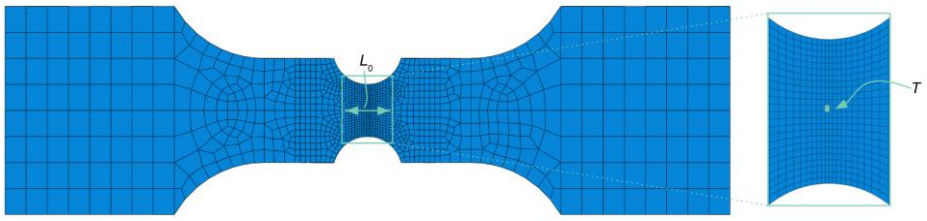

Fig.4: Finite element model of the NT3 specimen.

As illustrated in Figure 5, the intersections between the experimental curves and the results from simulations defined the Taylor-Quinney coefficient as a function of longitudinal engineering strain.

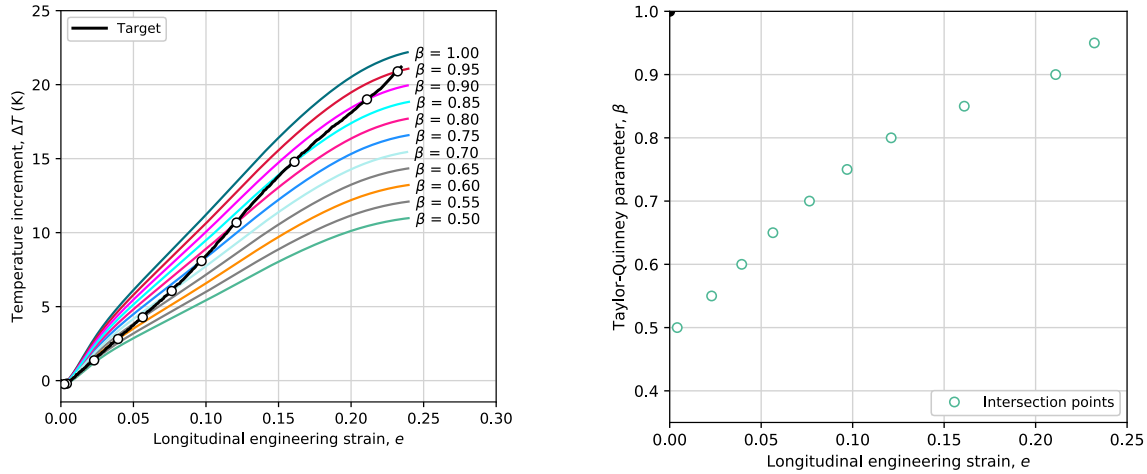

(a) (b)

Fig.5: (a) Illustration of how the initial guess for the optimization procedure is obtained and (b) the resulting Taylor-Quinney coefficient as a function of engineering strain.

The longitudinal engineering strain, found from L_0 in Figure 4, was then correlated with the equivalent plastic strain evaluated from the centermost element in the notch where the temperature was extracted, see Figure 4. This defined the initial input to LS-OPT, which was used to obtain the tabulated values of the Taylor-Quinney coefficient as a function of the equivalent plastic strain given in Figure 6.

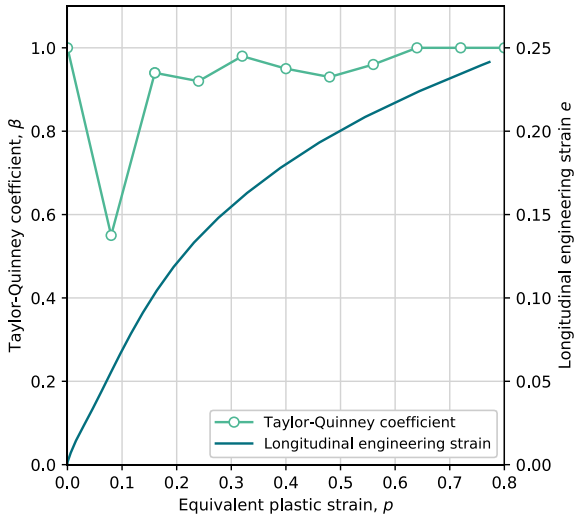

Fig.6: Optimized Taylor-Quinney coefficient as a function of equivalent plastic strain. Longitudinal engineering strain versus equivalent plastic strain is also shown.

A comparison of temperature increment and force versus longitudinal engineering strain is given in Figures 7(a) and 7(b), respectively, for a numerical simulation using the optimized set of parameters for the Taylor-Quinney coefficient. As shown, we obtain an excellent agreement between the simulated and measured temperature increments.

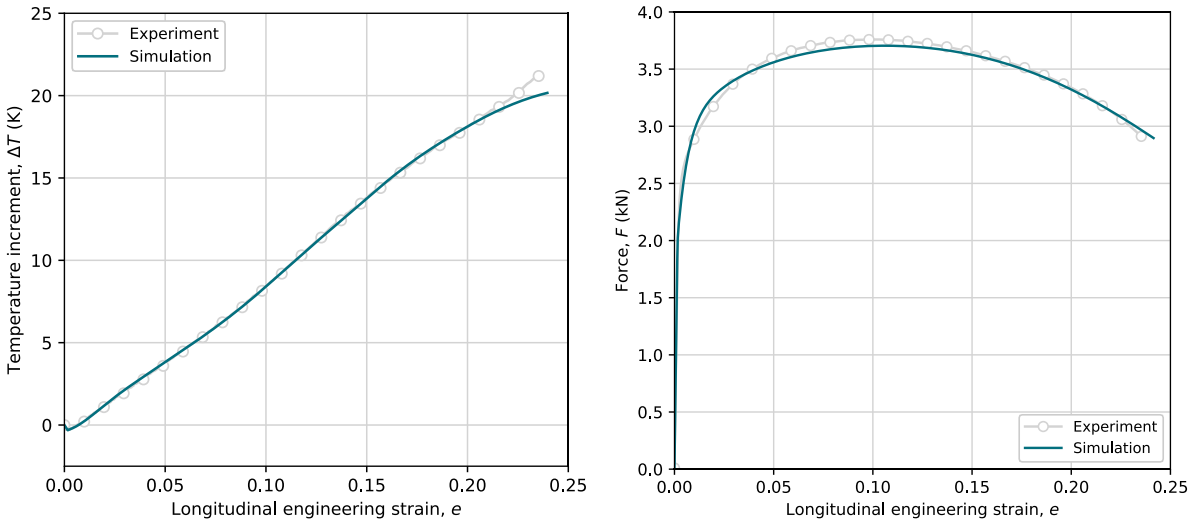

(a) (b)

Fig.7: (a) Comparison of temperature increment versus longitudinal engineering strain with the optimized Taylor-Quinney coefficients, and (b) force versus longitudinal engineering strain from experiment and simulation.

5 Summary

Notched tension tests on a 1.0 mm thick DP600 sheet steel material was conducted. Using both a digital camera and an infrared camera, the deformation on the surface of the specimen was correlated to the maximum surface temperature. A user subroutine was used to include the Taylor-Quinney coefficient as a function of the equivalent plastic strain, and the temperature increment versus the engineering strain was optimized against the experimental values from thermo-coupled simulations. Excellent agreement between simulation and experiment was obtained, both in terms of force vs. engineering strain, and temperature increment vs. engineering strain. Based on the numerical optimization, the Taylor-Quinney coefficient is found to vary quite significantly with the plastic strain and approaches unity with large plastic deformations due to a balance between storage and annihilation of dislocations. This variation of the Taylor-Quinney coefficient can be explained from thermodynamics and an analytical expression for $\beta(p)$ is derivable using the constitutive model adopted in this work.

6 References

[1] Taylor, G.I., Quinney, H.: "The latent energy remaining in a metal after cold working", Proceedings of the Royal Society of London, 307–326, 1934.

[2] Longère, P., Dragon, A..: "Evaluation of the inelastic heat fraction in the context of microstructure-supported dynamic plasticity modelling", International Journal of Impact Engineering, 992–999, 2008.

[3] Dumoulin, S., Louche, H., Hopperstad, O.S., Børvik, T.: "Heat sources, energy storage and dissipation in high-strength steels: Experiments and modelling", European Journal of Mechanics – A/solids, 461–474, 2010.

[4] Potter, T., Toussaint, F., Louche, H., Vacher, P.: "Inelastic heat fraction estimation from two successive mechanical and thermal analyses and full-field measurements", European Journal of Mechanics – A/solids, 1–11, 2013.

[5] Knysh, P., Korkolis, Y.P.: "Determination of the fraction of plastic work converted into heat in metals", Mechanics of Materials, 71–80, 2015.

[6] Rittel, D., Zhang, L.H., Osovski, S.: "The dependence of the Taylor-Quinney coefficient on the dynamic loading mode", Journal of the Mechanics and Physics of Solids, 96–114, 2017.

[7] ISO22007–4:2008, Plastics – Determination of Thermal Conductivity and Thermal Diffusivity – Part 4: Laser Flash Method, 2008.

[8] Hershey, A.V.: "The plasticity of an isotropic aggregate of anisotropic face-centered cubic crystals", Journal of Applied Mechanics, 241–249, 1954.

[9] Hosford, W.F.: "A generalized isotropic yield criterion", Journal of Applied Mechanics, 607–609, 1972.
[10] Børvik, T., Hopperstad, O.S., Berstad, T., Langseth, M.: "A computational model of viscoplasticity and ductile damage for impact and penetration", Europen Journal of Mechanics – A/Solids, 685–712, 2001.
[11] Miehe, C.: "Entropic thermoelasticity at finite strains. Aspects of the formulation and numerical implementation", Computer Methods in Applied Mechanics and Engineering, 243–269 , 1995.
[12] Johnsen, J., Clausen, A.H., Grytten, F., Benallal, A., Hopperstad, O.S.: "A thermo-elasto-viscoplastic constitutive model for polymers", Journal of the Mechanics and Physics of Solids, 681–701, 2019.